*Laser and Particle Beams* (2005), *23*, 321–325. Printed in the USA.

DOI: 10.1017/S0263034605050457

# Laser interactions with low-density plastic foams*

J. LIMPOUCH,[1,5] N.N. DEMCHENKO,[2] S.YU. GUS'KOV,[2] A.I. GROMOV,[2] M. KALAL,[1] A. KASPERCZUK,[3] V.N. KONDRASHOV,[4] E. KROUSKY,[5] K. MASEK,[5] M. PFEIFER,[5] P. PISARCZYK,[6] T. PISARCZYK,[3] K. ROHLENA,[5] V.B. ROZANOV,[2] M. SINOR,[1] AND J. ULLSCHMIED[7]

[1]Czech Technical University in Prague, FNSPE, Prague, Czech Republic
[2]P.N. Lebedev Physical Institute of the Russian Academy of Sciences, Moscow, Russia
[3]Institute of Plasma Physics & Laser Microfusion, Warsaw, Poland
[4]Troitsk Institute of Innovation and Thermonuclear Research, Troitsk, Russia
[5]Institute of Physics, AS CR, Prague, Czech Republic
[6]Warsaw University of Technology, ICS, Warsaw, Poland
[7]Institute of Plasma Physics, AS CR, Prague, Czech Republic

(RECEIVED 30 November 2004; ACCEPTED 10 December 2004)

**Abstract**

Interactions of sub-nanosecond pulses of kJ-class iodine laser "PALS" with low-density foams and acceleration of Al foils by the pressure of the heated foam matter are investigated here, both experimentally and theoretically. X-ray streak camera is used for evaluation of the speed of energy transfer through the porous foam material. The shock-wave arrival on the rear side of the target is monitored by optical streak camera. Accelerated foil velocities, measured by three-frame optical interferometers, and shadowgraphs, reach up to $10^7$ cm/s. The accelerated foil shape is smooth without any signature of small-scale structures present in the incident laser beam. Conversion efficiencies as high as 14% of the laser energy into the kinetic energy of Al foil are derived. Experimental results compare well with our two-dimensional hydrodynamics simulations and with an approximate analytical model.

**Keywords:** Laser-imprint smoothing; Laser-produced plasma; Low-density plastic foams; Shock wave propagation; Thermal transport

## 1. INTRODUCTION

The success of inertial fusion energy depends, to a large degree, on a detailed understanding of material properties under extreme conditions, and the ability to manufacture sophisticated targets (Borisenko *et al*., 2003; Sadot *et al*., 2003). Laser interactions with low-density plastic foams of supercritical density, with electron density $n_e$ in the fully ionized and homogenized foam, greater than the laser critical density, are important, as foam layers can be used for improvement of the spherical symmetry of direct-drive inertial fusion. Most approaches to implosion symmetry improvement are based on smoothing of laser imprint by thermal conductivity, in a relatively thick, relatively hot low-density outer layer of the target (Desselberger *et al*., 1992; Gus'kov *et al*., 1995; Gus'kov, 2005). An alternative approach to the mitigation of laser imprint is based on density tailoring of a layered target, consisting of low-density porous matter on top of a higher-density payload. A distant laser prepulse is used here as a shaping pulse that can provide impedance matching between foam and payload, and thus, Rayleigh-Taylor instability is suppressed (Metzler *et al*., 1999). While many experiments (Hall *et al*., 2002) use foams with micron or submicron pore size, interactions of laser pulses several nanosecond long, with foams of typical pore, and radius comparable or greater than 10 $\mu$m, was studied in other experiments (Gus'kov *et al*., 1996, 1999, 2000; Caruso *et al*., 2000). This study succeeds our previous work (Kalal *et al*., 2003), and the distinctive feature of these experiments is the interaction of subnanosecond laser pulses with foams containing large pores, when laser pulse is shorter than the time needed for full homogenization of the foam matter.

The main goal of our work is to study energy transport through low-density porous matter and to demonstrate a sufficient efficiency of thin foil acceleration, together with a substantial smoothing effect of the low-density foam absorber. The experimental setup will be explained in Section 2, while the results of X-ray and optical diagnostics are presented

Address correspondence and reprint requests to: J. Limpouch, Faculty of Nuclear Sciences and Physical Engineering CTU, Břehová 7, 115 19 Prague, Czech Republic. E-mail: limpouch@siduri.fjfi.cvut.cz
*This paper was presented at the 28th ECLIM conference in Rome, Italy.

and discussed in Section 3. Our two-dimensional hydrodynamic simulations are described in Section 4, where analytical estimates are also presented, and compared with experiments and simulations in Section 5. The conclusions are drawn and discussed in the last section.

## 2. EXPERIMENTAL SETUP

Experiments were conducted on the PALS iodine laser facility in Prague (Jungwirth *et al*., 2001; Jungwirth, 2005). The laser provided 400 ps (FWHM) pulses with energy up to 600 J at the basic frequency ($\lambda_1 = 1.32$ $\mu$m). The laser was incident normally on the target; the best radius focus spot was $R_L \approx 40$ $\mu$m. Here, the target was placed out of the best focus, and the laser spot radius $R_L \approx 150$ $\mu$m was used. Thus, the laser spot radius, $R_L$, is large compared to the pore diameter $D_p$. Laser irradiances were varied from $I \approx 10^{14}$ W/cm$^2$ to $I \approx 10^{15}$ W/cm$^2$. No method of optical smoothing was used, the laser beam focus was not quite uniform, and contained small-scale intensity non-uniformities.

Several types of foam targets were used. Most experiments were done with thick layers of polystyrene foam, with density in the range of 8–10 mg/cm$^3$, and typical pore diameter, $D_p \approx 50$–$70$ $\mu$m. Other polystyrene foams of density $\rho \approx 30$ mg/cm$^3$, with pore diameter $D_p \approx 10$ $\mu$m, and also of $\rho \approx 20$ mg/cm$^3$, and $D_p \approx 5$ $\mu$m, as well as polyvinylalcohol (PVA) foam of density $\rho \approx 5$ mg/cm$^3$, and of typical pore diameter $D_p \approx 5$ $\mu$m were used. A 2 or 0.8 $\mu$m thick aluminum foil was placed at the foam rear side in the majority of foam targets.

The diagnostic system included observation of target emission and target optical probing. Side-view slit image of plasma emission in the X-ray region (photon energy $> 1.5$ keV) was observed, with the KENTECH (low magnification) X-ray streak camera. The temporal resolution was either 30 or 70 ps, spatial resolution of 50 $\mu$m, was in the direction normal to the target surface (target depth). We present here also preliminary results on measurement of shock wave arrival at the target rear side via self-emission observed by optical streak camera. Optical interferometer and shadowgraphs were carried out by means of a three-frame interferometer system with automated image processing technique, described in detail by Pisarczyk *et al*. (1994). Each of the three recording channels was equipped with a CCD camera (Pulnix TM-1300), with a matrix of 1300 $\times$ 1030 pixels. The diagnostic system used a probing beam at the third harmonic frequency with similar, but slightly shorter pulse duration than that of the main beam. Interferogram processing included parasitic noise filtering, comparison of object and reference interferograms, and a subsequent reconstruction of radial electron density distributions.

## 3. EXPERIMENTAL RESULTS

The target self-emission was imaged (magnified 11-fold) by 50 $\mu$m wide slit, providing a spatial resolution along the target depth, on the entrance slit of X-ray streak camera. The recording channel included 17 $\mu$m of Mylar and 40 nm of aluminum, the transmission was negligible for photons of energy $\leq$1.1 keV, while the transmission was approximately 20% for 1.7 keV photons. As plastic foams containing only light elements were used, the amount of X-ray emission was rather low. The only usable pictures (weak, but significantly above X-ray streak sensitivity limit) were recorded for the foams with the largest pore diameter (50–70 $\mu$m). From the recordings presented in Figure 1, the upper estimate of the laser penetration depth is about 120 $\mu$m of the immediately heated layer. The laser penetration is consequently no more than two pore layers in this foam. Later, heat wave propagates into the foam material with velocity of approximately $1.4 \times 10^7$ cm/s, and the rear side of the heated X-ray emitting area is denoted by a solid white line in Figure 1. The X-ray signal lasts for nearly 3 ns, the X-ray emitting zone covers only about two-thirds of the foam thickness, and no emission near the Al foil at the target rear side is detected.

Experimental sequences of three interferometric pictures taken in one laser shot are presented in Figure 2. A sharp rear boundary of 400 $\mu$m-thick polystyrene target with 2 $\mu$m Al foil is observed, with no signs of low density plasma behind

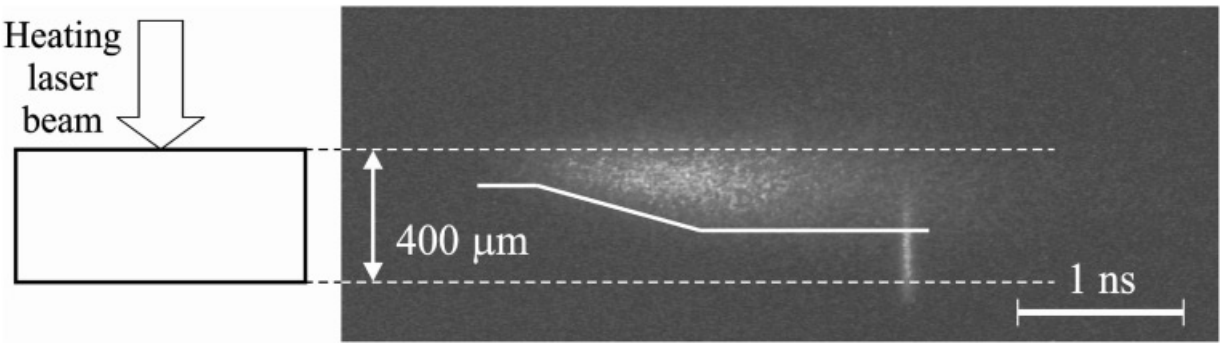


**Fig. 1.** X-ray streak record of lateral slit picture of interaction of 400 ps iodine laser ($\lambda = 1.32$ $\mu$m) pulse of energy 92 J and beam radius 150 $\mu$m with 400 $\mu$m thick polystyrene foam of density $\rho \approx 9$ mg/cm$^3$ and pore diameter $D_p \approx 50$–$70$ $\mu$m, 2 $\mu$m thick Al foil is placed at the target rear side.

https://doi.org/10.1017/S0263034605050457 Published online by Cambridge University Press

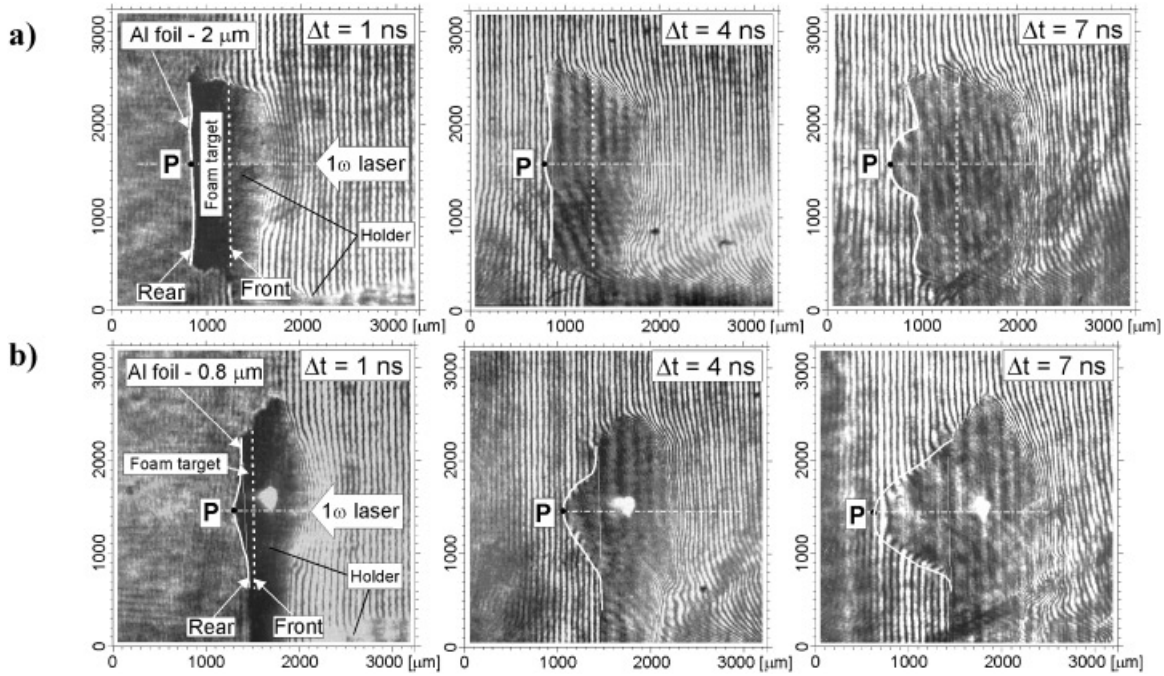


**Fig. 2.** Sequence of 3 interferograms recorded in one shot in time instants 1, 4, and 7 ns after the main 400 ps FWHM laser pulse maximum. Laser wavelength 1.32 $\mu$m and beam radius 150 $\mu$m on the targets. Parasitic effects of the target holder are denoted in the left pictures. (**a**) Polystyrene foam of $\rho \sim 9$ mg/cm$^3$, $D_p \sim 50$–70 $\mu$m, 400 $\mu$m thick and 2 $\mu$m thick Al foil at its rear side. Laser energy 173 J. (**b**) PVA foam of $\rho \sim 5$ mg/cm$^3$, $D_p \sim 5$ $\mu$m, 100 $\mu$m thick and 0.8 $\mu$m thick Al foil at its rear side. Laser energy was 238 J.

the target. On the other hand, 0.8 $\mu$m-thick Al foil at the rear side of 100 $\mu$m-thick PVA foam is heated and its expansion is later apparent.

The position of point *P* (rear side opposite to the laser beam centre) is measured with the precision of 5–10 $\mu$m; the results are summarized in Figure 3. The speed of the accelerated Al foil can be determined from the difference in point *P* positions in different frames. The speed of accelerated foil grows with the laser energy. Foil acceleration during the laser pulse is inferred for 100 $\mu$m thick PVA foam. For 400 $\mu$m-thick polystyrene foams, the shock wave reaches the foil only 2 to 4 ns after the laser pulse, and the delay decreases with laser energy. The above delay is larger by about 2 ns than in simulations for homogeneous material of the same density as the foam, and the difference is tentatively explained by foam homogenization process.

In order to verify the measurement of time and form of the shock wave arrival on the target rear side, we conducted preliminary experiments where self-emission in the normal direction from the target rear side was imaged (with magnification of 10) on the entrance slit of an optical streak camera. The result is presented in Figure 4 where the absolute timing of the shock wave arrival is determined by the fiducial in the left upper corner. The shock wave arrival delay grows smoothly with the distance from the central point. No macroscopic spatial features are registered, which is also consistent with smooth shape of the accelerated part of the foil observed in optical interferometer. This preliminary measurement was carried out during other experiments on the PALS laser and third harmonics frequency of iodine laser was used. Consequently, direct comparison of this measurement with the other results presented here is not possible due to different experimental conditions. However, the delay in shock wave arrival on the target rear side is considerably smaller than in interferometric measurements

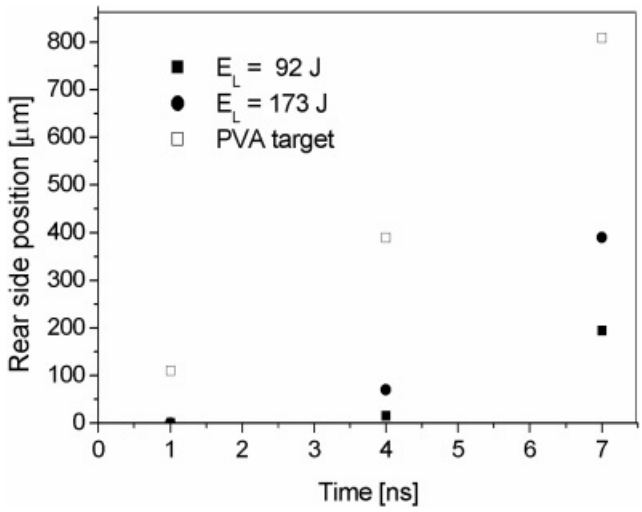


**Fig. 3.** Experimentally measured position of point P versus time after the laser pulse maximum for two laser energies and 2 $\mu$m Al foil on polystyrene foam of $\rho \approx 8$–10 mg/cm$^3$, pore diameter $D_p \approx 50$–70 $\mu$m and thickness $\Delta = 400$ $\mu$m. Points are also plotted for 0.8 $\mu$m Al foil on PVA foam of $\rho \approx 5$ mg/cm$^3$, $D_p \approx 5$ $\mu$m, $\Delta = 100$ $\mu$m and laser energy 238 J.

https://doi.org/10.1017/S0263034605050457 Published online by Cambridge University Press

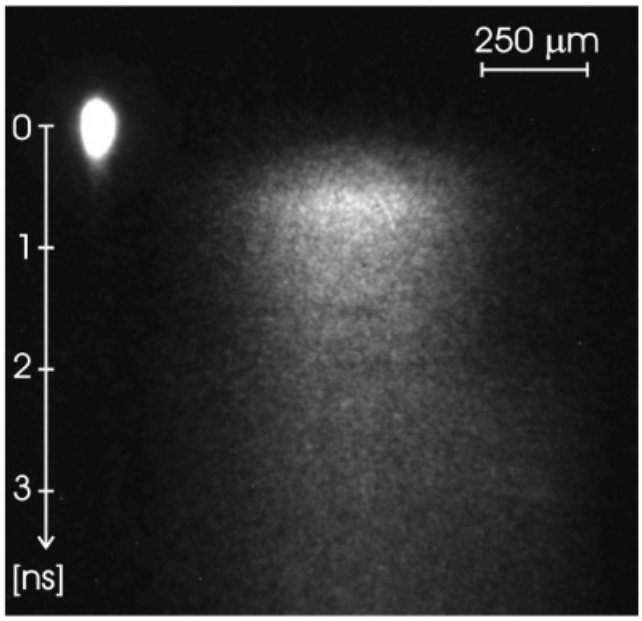


**Fig. 4.** Optical streak record of self-emission of the target rear side with fiducial in the upper left corner. Third harmonic of iodine laser pulse (wavelength $\lambda = 432$ nm, energy $E_L = 264$ J, pulse length 350 ps FWHM) is focused to a spot of radius 200 $\mu$m on 700 $\mu$m thick polystyrene foam of density $\rho \approx 9$ mg/cm$^3$ and pore diameter $D_p \approx 50$–70 $\mu$m, 5 $\mu$m thick Al foil is placed at the target rear side. Time zero denotes laser pulse maximum.

conducted for the laser basic frequency. This is tentatively explained by the fact that the foam used is underdense for the third harmonic of iodine laser while it is overdense for the laser basic frequency.

## 4. COMPUTATIONAL SIMULATIONS AND ANALYTICAL MODEL

Simulations were performed in cylindrical geometry by two-dimensional Lagrangian hydrodynamics code ATLANT-HE, including advanced treatment of laser propagation and absorption (Iskakov *et al*., 2003). The code does not take into account fine scale structure of the foam and thus the time of the hydrothermal wave transit through the foam may be underestimated.

The calculated laser absorption was approximately 50%. Plasma radius essentially exceeds the laser beam radius on the target (radius of laser produced plasma reaches approximately 1000 $\mu$m for laser beam of radius 150 $\mu$m on the target) due to fast lateral heat transport in the low-density porous matter. A smooth shape of the accelerated foil is observed in simulations with the width considerably larger than the laser beam diameter. The fast electrons do not preheat unevaporated Al layer in simulations significantly for the laser intensities $\leq 10^{15}$ W/cm$^2$.

Analytical model is based on the assumption of spherical hydrothermal wave (Gus'kov *et al*., 2000) propagating from laser absorption region. Time instants when the hydrothermal wave reaches the target rear side are in a good agreement with numerical simulations. However, the experimental time delays are about 2 ns greater for 400 $\mu$m thick polystyrene foam. According to our opinion, such a fact is caused by the direct influence of the initial structure of foam on the target dynamics. The pressure accelerating the Al foil is calculated and the derived hydrodynamic efficiency is $\eta \approx 0.12$.

**Table 1.** *$(CH)_n$ is 400 $\mu$m thick polystyrene foam of density 9 mg/cm$^3$ with 2 $\mu$m Al foil and PVA is 100 $\mu$m thick PVA foam of density 5 mg/cm$^3$ with 0.8 $\mu$m Al foil. Experimental and simulation velocities are represented by average values in the interval 4–7 ns after the laser maximum*

| Energy | Target | $v_{exp}$ (cm/s) | $v_{simul}$ | $V_{max}$ |
|---|---|---|---|---|
| 92 J | $(CH)_n$ | $6.0 \times 10^6$ | $4.9 \times 10^6$ | $4.8 \times 10^6$ |
| 173 J | $(CH)_n$ | $8.0 \times 10^6$ | $8.2 \times 10^6$ | $6.7 \times 10^6$ |
| 238 J | $(CH)_n$ | — | $1.1 \times 10^7$ | $8.2 \times 10^6$ |
| 238 J | PVA | $1.4 \times 10^7$ | $3.5 \times 10^7$ | $1.32 \times 10^7$ |

The foil velocities measured in the experiment, calculated in our simulations, and via analytical model are compared in Table 1. The Al foil in PVA foam target is heated up to 800 eV in the simulations and its expansion leads to an excessive velocity of the rear boundary.

## 5. CONCLUSIONS

Interactions of laser beam of iodine laser "PALS" with low-density foam targets have been investigated, both experimentally, and theoretically. The speed of the heat wave inside polystyrene foam was estimated to be $\sim 1.4 \times 10^7$ cm/s from the X-ray streak measurements.

Velocities of the accelerated foil at the target rear side, measured by three-frame optical interferometer, are in a good agreement with our two-dimensional hydrodynamic calculations, and with analytical model. However, a delay in the shock wave propagation in the foam is observed in our experiments in comparison with our theoretical calculations that do not take foam structure into account. This is explained here by the phenomenon of non-equilibrium foam homogenization. This delay may influence laser imprint mitigation. A smooth arrival of the shock wave on the target rear side detected by optical streak camera is in agreement with a smooth shape of the accelerated foil observed interferometrically.

## ACKNOWLEDGMENTS

This work was partly funded by project INTAS-01-572 and by IAEA Research Project No. 11655/RBF. Partial support of the Czech participants by the Czech Ministry of Education, Youth and Sports under project LNA00100 "Laser Plasma Research Centre" is gratefully acknowledged. The authors thank Dr. Dimitri Batani for his kind assistance in preliminary optical streak measurements, and to the PALS staff for an excellent experimental support.

## REFERENCES


Borisenko, N.G., Akunets, A.A., Bushuev, V.S., Dorogotovtsev, V.M. & Merkuliev, Yu.A. (2003). Motivation and fabrication methods for inertial confinement fusion and inertial fusion energy targets. *Laser Part. Beams* **21**, 505–509.

Caruso, A., Strangio, C., Gus'kov, S.Yu. & Rozanov, V.B. (2000). Interaction experiments of laser light with low density supercritical foams at the AEEF ABC facility. *Laser Part. Beams* **18**, 25–34.

Desselberger, M., Jones, M.W., Edwards, J., Dunne, M. & Willi, O. (1992). Nonuniformity imprint on the ablation surface of laser-irradiated targets. *Phys. Rev. Lett.* **68**, 1539–1542.

Gus'kov, S.Yu., Gromov, A.I., Merkul'ev, Yu.A., Rozanov, V.B., Nikishin, V.V., Tishkin, V.F., Zmitrenko, N.V., Gavrilov, V.V., Gol'tsov, A.A., Kondrashov, V.N., Kovalsky, N.V., Pergament, M.I., Garanin, S.G., Kirillov, G.A., Sukharev, S.A., Caruso, A. & Strangio, C. (2000). Nonequilibrium laser-produced plasma of volume-structured media and ICF applications. *Laser Part. Beams* **18**, 1–10.

Gus'kov, S.Yu., Zmitrenko, N.V. & Rozanov, V.B. (1995). Laser-greenhouse thermonuclear target with distributed absorption of laser energy. *JETP* **81**, 296–304.

Gus'kov, S.Yu. (2005). Thermonuclear gain and parameters of fast ignition ICF-targets. *Laser Part. Beams* **23**, 255–260.

Gus'kov, S.Yu., Kas'anov, Yu.S., Koshevoi, M.O., Rozanov, V.B., Rupasov, A.A. & Shikanov A.S. (1999). Scattering and transmission of laser radiation at the heating of low-density foam targets. *Laser Part. Beams* **17**, 287–291.

Gus'kov, S.Yu., Koshevoi, M.O., Rozanov, V.B., Rupasov, A.A., Shikanov, A.S. & Kas'anov, Yu.S. (1996). Dynamics of high-temperature plasma formation during laser irradiation of three-dimensionally structured, low-density matter. *JETP Letters* **64**, 502–508.

Hall, T., Batani, D., Nazarov, W., Koenig, M. & Benuzzi, A. (2002). Recent advances in laser–plasma experiments using foams. *Laser Part. Beams* **20**, 303–316.

Iskakov, A.B., Demchenko, N.N., Lebo, I.G., Rozanov, V.B. & Tishkin, V.F. (2003). 2D Lagrangian code "ATLANT-HE" for simulation of laser-plasma interaction with allowance for hot electron generation and transport. *Proc. SPIE* **5228**, 143–150.

Jungwirth, K. (2005). Recent highlights of the PALS research programme. *Laser Part. Beams* **23**, 177–182.

Jungwirth, K., Cejnarova, A., Juha, L., Kralikova, B., Krasa, J., Krousky, E., Krupickova, P., Laska, L., Masek, K., Mocek, T., Pfeifer, M., Prag, A., Renner, O., Rohlena, K., Rus, B., Skala, J., Straka, P. & Ullschmied, J. (2001). The Prague Asterix Laser System. *Phys. Plasmas* **8**, 2495–2501.

Kalal, M., Limpouch, J., Krousky, E., Masek, K., Rohlena, K., Straka, P., Ullschmied, J., Kasperczuk, A., Pisarczyk, T., Gus'kov, S.Yu., Gromov, A.I., Rozanov, V.B. & Kondrashov, V.N. (2003). Thermal smoothing by laser-produced plasma of porous matter. *Fusion Sci. Technol.* **43**, 275–281.

Metzler, N., Velikovich, A.L. & Gardner, J.H. (1999). Reduction of early-time perturbation growth in ablatively driven laser targets using tailored density profiles. *Phys. Plasmas* **6**, 3283–3295.

Pisarczyk, T., Arendzikowski, R., Parys, P. & Patron, Z. (1994). Polari-interferometer with automatic images processing for laser plasma diagnostics. *Laser Part. Beams* **12**, 549–562.

Sadot, O., Rikanati, A., Oron, D., Ben-Dor, G. & Shvarts, D. (2003). An experimental study of the high Mach number and high initial-amplitude effects on the evolution of the single-mode Richtmyer–Meshkov instability. *Laser Part. Beams* **21**, 341–346.


https://doi.org/10.1017/S0263034605050457 Published online by Cambridge University Press